

COMPUTATION OF NONLINEAR NORMAL MODES, PART I: NUMERICAL CONTINUATION IN MATLAB

M. Peeters, R. Vigié, G. Sérandour, G. Kerschen, J.C. Golinval

Structural Dynamics Research Group

Aerospace and Mechanical Engineering Department

University of Liège, Liège, Belgium

m.peeters,r.viguie,g.serandour,g.kerschen,jc.golinval@ulg.ac.be

Abstract

The concept of nonlinear normal modes (NNMs) is discussed in the present paper and its companion, Part II. Because there is virtually no application of the NNMs to large-scale engineering structures, these papers are an attempt to highlight one aspect that might drive their development in the future. Specifically, we argue that numerical methods for the continuation of periodic solutions pave the way for an effective and practical computation of NNMs. In this context, we show that the NNM computation is possible with limited implementation effort. The proposed algorithm, implemented in MATLAB, relies on two main techniques, namely a shooting procedure and a method for the continuation of NNM motions. The algorithm is demonstrated using a 2DOF nonlinear system. A comparison with the results given by the AUTO software is achieved in Part II.

Key words

Nonlinear normal modes, periodic solution, numerical computation, shooting, continuation techniques.

1 Introduction

Nonlinear normal modes (NNMs) offer a solid theoretical and mathematical tool for interpreting a wide class of nonlinear dynamical phenomena, yet they have a clear and simple conceptual relation to the LNMs [Vakakis et al., 1996; Vakakis, 1997; Kerschen et al., 2008]. However, most structural engineers still view NNMs as a concept that is foreign to them, and they do not yet consider NNMs as a useful concept for structural dynamics. One reason supporting this statement is that most existing constructive techniques for computing NNMs are based on asymptotic approaches and rely on fairly involved mathematical developments.

There have been very few attempts to compute NNMs using numerical methods [Slater, 1996; Pesheck, 2000; Lee et al., 2005; Arquier, 2007]. Algorithms for the

continuation of periodic solutions are really quite sophisticated and advanced (see, e.g., [Seydel, 1994; Doedel, 2007]), and they have been extensively used for computing the forced response and limit cycles of nonlinear dynamical systems (see, e.g., [Touzé et al., 2007]). Interestingly, they have not been fully exploited for the computation of nonlinear modes.

The objective of this paper and its companion, Part II, is to support that these numerical algorithms pave the way for an effective and practical computation of NNMs. In the present paper, we show that the NNM computation is possible with limited implementation effort. The proposed algorithm, implemented in MATLAB, relies on two main techniques, namely a shooting procedure and a method for the continuation of NNM motions. The algorithm is demonstrated using a 2DOF nonlinear system. In Part II, the same study is carried out using the AUTO software.

2 Nonlinear Normal Modes (NNMs)

A detailed description of NNMs and their fundamental properties (e.g., frequency-energy dependence, bifurcations and stability) is given in [Vakakis et al., 1996; Vakakis, 1997; Kerschen et al., 2008]. For completeness, the two main definitions of an NNM are briefly reviewed in this section.

The free response of discrete conservative mechanical systems with n degrees of freedom (DOFs) is considered, assuming that continuous systems (e.g., beams, shells or plates) have been spatially discretized using the finite element method. The equations of motion are

$$\mathbf{M} \ddot{\mathbf{x}}(t) + \mathbf{K} \mathbf{x}(t) + \mathbf{f}_{nl} \{\mathbf{x}(t), \dot{\mathbf{x}}(t)\} = 0 \quad (1)$$

where \mathbf{M} is the mass matrix; \mathbf{K} is the stiffness matrix; \mathbf{x} , $\dot{\mathbf{x}}$ and $\ddot{\mathbf{x}}$ are the displacement, velocity and acceleration vectors, respectively; \mathbf{f}_{nl} is the nonlinear restoring force vector.

There exist two main definitions of an NNM in the literature due to Rosenberg and Shaw and Pierre:

1. Targeting a straightforward nonlinear extension of the linear normal mode (LNM) concept, Rosenberg defined an NNM motion as a *vibration in unison* of the system (i.e., a synchronous periodic oscillation).
2. To provide an extension of the NNM concept to damped systems, Shaw and Pierre defined an NNM as a two-dimensional invariant manifold in phase space. Such a manifold is invariant under the flow (i.e., orbits that start out in the manifold remain in it for all time), which generalizes the invariance property of LNMs to nonlinear systems.

At first glance, Rosenberg's definition may appear restrictive in two cases. Firstly, it cannot be easily extended to nonconservative systems. However, the damped dynamics can often be interpreted based on the topological structure of the NNMs of the underlying conservative system [Kerschen et al., 2008]. Secondly, in the presence of internal resonances, the NNM motion is no longer synchronous, but it is still periodic.

In the present study, an NNM motion is therefore defined as a (*non-necessarily synchronous*) *periodic motion* of the undamped mechanical system (1). As we will show, this extended definition is particularly attractive when targeting a numerical computation of the NNMs. It enables the nonlinear modes to be effectively computed using algorithms for the continuation of periodic solutions.

3 Numerical Computation of NNMs

The numerical method proposed here for the NNM computation relies on two main techniques, namely a shooting technique and the pseudo-arclength continuation method. A detailed description of the algorithm is given in [Peeters et al., 2008].

3.1 Shooting Method

The equations of motion of system (1) can be recast into state space form

$$\dot{\mathbf{z}} = \mathbf{g}(\mathbf{z}) \quad (2)$$

where $\mathbf{z} = [\mathbf{x}^* \quad \dot{\mathbf{x}}^*]^*$ is the $2n$ -dimensional state vector, and star denotes the transpose operation, and

$$\mathbf{g}(\mathbf{z}) = \begin{pmatrix} \dot{\mathbf{x}} \\ -\mathbf{M}^{-1} [\mathbf{K}\mathbf{x} + \mathbf{f}_{nl}(\mathbf{x}, \dot{\mathbf{x}})] \end{pmatrix} \quad (3)$$

is the vector field. The solution of this dynamical system for initial conditions $\mathbf{z}(0) = \mathbf{z}_0 = [\mathbf{x}_0^* \quad \dot{\mathbf{x}}_0^*]^*$ is written as $\mathbf{z}(t) = \mathbf{z}(t, \mathbf{z}_0)$ in order to exhibit the dependence on the initial conditions, $\mathbf{z}(0, \mathbf{z}_0) = \mathbf{z}_0$. A solution $\mathbf{z}_p(t, \mathbf{z}_{p0})$ is a periodic solution of the autonomous system (2) if $\mathbf{z}_p(t, \mathbf{z}_{p0}) = \mathbf{z}_p(t + T, \mathbf{z}_{p0})$, where T is the minimal period.

The NNM computation is carried out by finding the periodic solutions of the governing nonlinear equations

of motion (2). In this context, the *shooting method* is probably the most popular numerical technique. It solves numerically the two-point boundary-value problem defined by the periodicity condition

$$\mathbf{H}(\mathbf{z}_{p0}, T) \equiv \mathbf{z}_p(T, \mathbf{z}_{p0}) - \mathbf{z}_{p0} = \mathbf{0} \quad (4)$$

$\mathbf{H}(\mathbf{z}_0, T) = \mathbf{z}(T, \mathbf{z}_0) - \mathbf{z}_0$ is called the *shooting function* and represents the difference between the initial conditions and the system response at time T . Unlike forced motion, the period T of the free response is not known a priori.

The shooting method consists in finding, in an iterative way, the initial conditions \mathbf{z}_{p0} and the period T that realize a periodic motion. To this end, the method relies on direct numerical time integration and on the Newton-Raphson algorithm.

Starting from some assumed initial conditions $\mathbf{z}_{p0}^{(0)}$, the motion $\mathbf{z}_p^{(0)}(t, \mathbf{z}_{p0}^{(0)})$ at the assumed period $T^{(0)}$ can be obtained by numerical time integration methods (e.g., Runge-Kutta or Newmark schemes). In general, the initial guess $(\mathbf{z}_{p0}^{(0)}, T^{(0)})$ does not satisfy the periodicity condition (4). A Newton-Raphson iteration scheme is therefore to be used to correct an initial guess and to converge to the actual solution. The corrections $\Delta\mathbf{z}_{p0}^{(0)}$ and $\Delta T^{(0)}$ are found by expanding the nonlinear function

$$\mathbf{H}(\mathbf{z}_{p0}^{(0)} + \Delta\mathbf{z}_{p0}^{(0)}, T^{(0)} + \Delta T^{(0)}) = 0 \quad (5)$$

in Taylor series and neglecting higher-order terms (H.O.T.).

The phase of the periodic solutions is not fixed. If $\mathbf{z}(t)$ is a solution of the autonomous system (2), then $\mathbf{z}(t + \Delta t)$ is geometrically the same solution in state space for any Δt . Hence, an additional condition, termed the *phase condition*, has to be specified in order to remove the arbitrariness of the initial conditions. This is discussed in detail in [Peeters et al., 2008].

In summary, an isolated NNM is computed by solving the augmented two-point boundary-value problem defined by

$$\mathbf{F}(\mathbf{z}_{p0}, T) \equiv \begin{cases} \mathbf{H}(\mathbf{z}_{p0}, T) = 0 \\ h(\mathbf{z}_{p0}) = 0 \end{cases} \quad (6)$$

where $h(\mathbf{z}_{p0}) = 0$ is the phase condition.

3.2 Continuation of Periodic Solutions

Due to the frequency-energy dependence, the modal parameters of an NNM vary with the total energy. An NNM family, governed by equations (6), therefore traces a curve, termed an NNM branch, in the $(2n + 1)$ -dimensional space of initial conditions and period (\mathbf{z}_{p0}, T) . Starting from the corresponding LNM

at low energy, the computation is carried out by finding successive points (\mathbf{z}_{p0}, T) of the NNM branch using methods for the *numerical continuation* of periodic motions (also called *path-following methods*) [Seydel, 1994]. The space (\mathbf{z}_{p0}, T) is termed the continuation space.

Different methods for numerical continuation have been proposed in the literature. The so-called pseudo-arclength continuation method is used herein.

Starting from a known solution $(\mathbf{z}_{p0,(j)}, T_{(j)})$, the next periodic solution $(\mathbf{z}_{p0,(j+1)}, T_{(j+1)})$ on the branch is computed using a *predictor step* and a *corrector step*.

Predictor step

At step j , a prediction $(\tilde{\mathbf{z}}_{p0,(j+1)}, \tilde{T}_{(j+1)})$ of the next solution $(\mathbf{z}_{p0,(j+1)}, T_{(j+1)})$ is generated along the tangent vector to the branch at the current point $\mathbf{z}_{p0,(j)}$

$$\begin{bmatrix} \tilde{\mathbf{z}}_{p0,(j+1)} \\ \tilde{T}_{(j+1)} \end{bmatrix} = \begin{bmatrix} \mathbf{z}_{p0,(j)} \\ T_{(j)} \end{bmatrix} + s_{(j)} \begin{bmatrix} \mathbf{p}_{z,(j)} \\ p_{T,(j)} \end{bmatrix} \quad (7)$$

where $s_{(j)}$ is the predictor stepsize. The tangent vector $\mathbf{p}_{(j)} = [\mathbf{p}_{z,(j)}^T \ p_{T,(j)}]^T$ to the branch defined by (6) is solution of the system

$$\begin{bmatrix} \frac{\partial \mathbf{H}}{\partial \mathbf{z}_{p0}} \Big|_{(\mathbf{z}_{p0,(j)}, T_{(j)})} & \frac{\partial \mathbf{H}}{\partial T} \Big|_{(\mathbf{z}_{p0,(j)}, T_{(j)})} \\ \frac{\partial h}{\partial \mathbf{z}_{p0}} \Big|_{(\mathbf{z}_{p0,(j)})} & 0 \end{bmatrix} \begin{bmatrix} \mathbf{p}_{z,(j)} \\ p_{T,(j)} \end{bmatrix} = \begin{bmatrix} \mathbf{0} \\ 0 \end{bmatrix} \quad (8)$$

with the condition $\|\mathbf{p}_{(j)}\| = 1$. The star denotes the transpose operator. This normalization can be taken into account by fixing one component of the tangent vector and solving the resulting overdetermined system using the Moore-Penrose matrix inverse; the tangent vector is then normalized to 1.

Corrector step

The prediction is corrected by a shooting procedure in order to solve (6) in which the variations of the initial conditions and the period are forced to be orthogonal to the predictor step. At iteration k , the corrections

$$\begin{aligned} \mathbf{z}_{p0,(j+1)}^{(k+1)} &= \mathbf{z}_{p0,(j+1)}^{(k)} + \Delta \mathbf{z}_{p0,(j+1)}^{(k)} \\ T_{(j+1)}^{(k+1)} &= T_{(j+1)}^{(k)} + \Delta T_{(j+1)}^{(k)} \end{aligned} \quad (9)$$

are computed by solving the overdetermined linear system using the Moore-Penrose matrix inverse

$$\begin{bmatrix} \frac{\partial \mathbf{H}}{\partial \mathbf{z}_{p0}} \Big|_{(\mathbf{z}_{p0,(j+1)}^{(k)}, T_{(j+1)}^{(k)})} & \frac{\partial \mathbf{H}}{\partial T} \Big|_{(\mathbf{z}_{p0,(j+1)}^{(k)}, T_{(j+1)}^{(k)})} \\ \frac{\partial h}{\partial \mathbf{z}_{p0}} \Big|_{(\mathbf{z}_{p0,(j+1)}^{(k)})} & 0 \\ \mathbf{p}_{z,(j)}^T & p_{T,(j)} \end{bmatrix} \begin{bmatrix} \Delta \mathbf{z}_{p0,(j+1)}^{(k)} \\ \Delta T_{(j+1)}^{(k)} \end{bmatrix} =$$

$$\begin{bmatrix} -\mathbf{H}(\mathbf{z}_{p0,(j+1)}^{(k)}, T_{(j+1)}^{(k)}) \\ -h(\mathbf{z}_{p0,(j+1)}^{(k)}) \\ 0 \end{bmatrix} \quad (10)$$

where the prediction is used as initial guess, i.e., $\mathbf{z}_{p0,(j+1)}^{(0)} = \tilde{\mathbf{z}}_{p0,(j+1)}$ and $T_{(j+1)}^{(0)} = \tilde{T}_{(j+1)}$. The last equation in (10) corresponds to the orthogonality condition for the corrector step.

This iterative process is carried out until convergence is achieved. The convergence test is based on the relative error of the periodicity condition:

$$\frac{\|\mathbf{H}(\mathbf{z}_{p0}, T)\|}{\|\mathbf{z}_{p0}\|} = \frac{\|\mathbf{z}_p(T, \mathbf{z}_{p0}) - \mathbf{z}_{p0}\|}{\|\mathbf{z}_{p0}\|} < \epsilon \quad (11)$$

where ϵ is the prescribed relative precision.

3.3 Algorithm for NNM computation

The algorithm proposed for the computation of NNM motions is a combination of shooting and pseudo-arclength continuation methods, as shown in Figure 1. It has been implemented in the MATLAB environment. Other features of the algorithm such as the step control, the reduction of the computational burden and the method used for numerical integration of the equations of motion are discussed in [Peeters et al., 2008].

So far, the NNMs have been considered as branches in the continuation space (\mathbf{z}_{p0}, T) . An appropriate graphical depiction of the NNMs is to represent them in a frequency-energy plot (FEP). This FEP can be computed in a straightforward manner: (i) the conserved total energy is computed from the initial conditions realizing the NNM motion; and (ii) the frequency of the NNM motion is calculated directly from the period.

4 Numerical Experiment

The NNM computation method is now demonstrated using a 2DOF system. More complex examples are considered in [Kerschen et al., 2008; Peeters et al., 2008], but due to space limitation, they are not described herein.

The governing equations of motion of the system are

$$\begin{aligned} \ddot{x}_1 + (2x_1 - x_2) + 0.5x_1^3 &= 0 \\ \ddot{x}_2 + (2x_2 - x_1) &= 0 \end{aligned} \quad (12)$$

The two NNMs of the underlying linear system are in-phase and out-of-phase modes for which the two DOFs vibrate with the same amplitude. The natural eigenfrequencies are $f_1 = 1/2\pi \simeq 0.159$ Hz and $f_2 = \sqrt{3}/2\pi \simeq 0.276$ Hz.

The FEP of this nonlinear system is shown in Figure 2. The evolution of NNM motions in the configuration space (i.e., the modal curves) are inset. The backbone of the plot is formed by two branches, which

represent in-phase ($S11+$) and out-of-phase ($S11-$) synchronous NNMs. They are the continuation of the corresponding LNMs. The letter S refers to symmetric periodic solutions for which the displacements and velocities of the system at half period are equal but with an opposite sign to those at time $t = 0$. The indices in the notations are used to mention that the two masses vibrate with the same dominant frequency. The FEP clearly shows that the nonlinear modal parameters, namely the modal curves and the corresponding frequencies of oscillation, have a strong dependence on the total energy in the system.

Another salient feature of NNMs is that they can undergo modal interactions through internal resonances. When carrying out the NNM computation at higher energy levels, Figure 3 shows that others branches of periodic solutions, termed *tongues*, bifurcate from the backbone branch $S11+$. For instance, unsymmetric periodic solutions are encountered and are denoted by a letter U . On these tongues, denoted Snm and Unm , there exist several dominant frequency components, which results in a $n:m$ internal resonance between the in-phase and out-phase NNMs. These additional branches correspond to internally resonant NNM motions, as opposed to fundamental NNM motions; they have no counterpart in linear systems.

Surprisingly, the ratio of the linear natural frequencies of the system is $\sqrt{3}$. Due to energy dependence, internal resonances can still be realized, because the frequency of the in-phase NNM increases less rapidly than that of the out-of-phase NNM. This clearly shows that NNMs can be internally resonant without necessarily having commensurate linear natural frequencies, a feature that is rarely discussed in the literature. This also underlines that important nonlinear phenomena can be missed when resorting to perturbation techniques, which are limited to small-amplitude motions.

5 Conclusion

In this paper, a numerical method for the computation of NNMs of mechanical structures was introduced. The approach targets the computation of the undamped modes of structures discretized by finite elements and relies on the continuation of periodic solutions. The procedure was demonstrated using a 2DOF system, and the NNMs were computed accurately in a fairly automatic manner. Complicated NNM motions were also observed, including a countable infinity of internal resonances and strong motion localization.

This method represents a first step toward a practical NNM computation with limited implementation effort. However, two important issues must be addressed adequately to develop a robust method capable of dealing with large, three-dimensional structures:

- (i) Fundamental NNMs with no linear counterparts (i.e., those that are not the direct extension of the LNMs) have not been discussed herein. These additional NNMs bifurcate from other modes, and a

robust branch switching strategy will be developed for their computation.

- (ii) The method relies on extensive numerical simulations and may be computationally intensive for large-scale finite element models. As a result, a further reduction of the computational cost is the next objective. To this end, a significant improvement is to use sensitivity analysis to obtain the Jacobian matrix as a by-product of the time integration of the current motion. An automatic time step control, which selects the most appropriate time step in view of the current dynamics, will also be considered to speed up the computations.

References

- Arquier, R. (2007) Une méthode de calcul des modes de vibrations non-linéaires de structures. *PhD Thesis*. Université de la Méditerranée, Marseille.
- Doedel, E. (2007). *AUTO, Software for Continuation and Bifurcation Problems in Ordinary Differential Equations*.
- Kerschen, G., Peeters, M., Golinval, J.C., Vakakis, A.F. (2008) Nonlinear normal modes, Part I: A useful framework for the structural dynamicist. *Mechanical Systems and Signal Processing*, submitted.
- Lee, Y.S., Kerschen, G., Vakakis, A.F., Panagopoulos, P.N., Bergman, L.A., McFarland, D.M. (2005) Complicated dynamics of a linear oscillator with a light, essentially nonlinear attachment. *Physica D*, **204**, pp. 41-69.
- Peeters, M., Vigié, R., Sérandour, G., Kerschen, G., Golinval, J.C. (2008) Nonlinear normal modes, Practical computation using numerical continuation techniques. *Mechanical Systems and Signal Processing*, submitted.
- Pesheck, E. (2000) Reduced-order modeling of nonlinear structural systems using nonlinear normal modes and invariant manifolds. *PhD Thesis*, University of Michigan, Ann Arbor.
- Seydel, R. (1994). *Practical Bifurcation and Stability Analysis, from Equilibrium to Chaos*. Springer-Verlag, 2nd Edition.
- Slater, J.C. (1996) A numerical method for determining nonlinear normal modes. *Nonlinear Dynamics*, **10**, pp. 19-30.
- Touzé, C. Amabili, A., Thomas, O. (2007) - Reduced-order models for large-amplitude vibrations of shells including in-plane inertia. In *Proceedings of the EUROMECH Colloquium on Geometrically Nonlinear Vibrations*. Porto, Portugal, July 2007.
- Vakakis, A.F., Manevitch, L.I., Mikhlin, Y.V., Pilipchuk, V.N., Zevin, A.A. (1996). *Normal Modes and Localization in Nonlinear Systems*. John Wiley & Sons. New York.
- Vakakis, A.F. (2008) Nonlinear normal modes and their applications in vibration theory: an overview. *Mechanical Systems and Signal Processing*, textbf11, pp. 3-22.

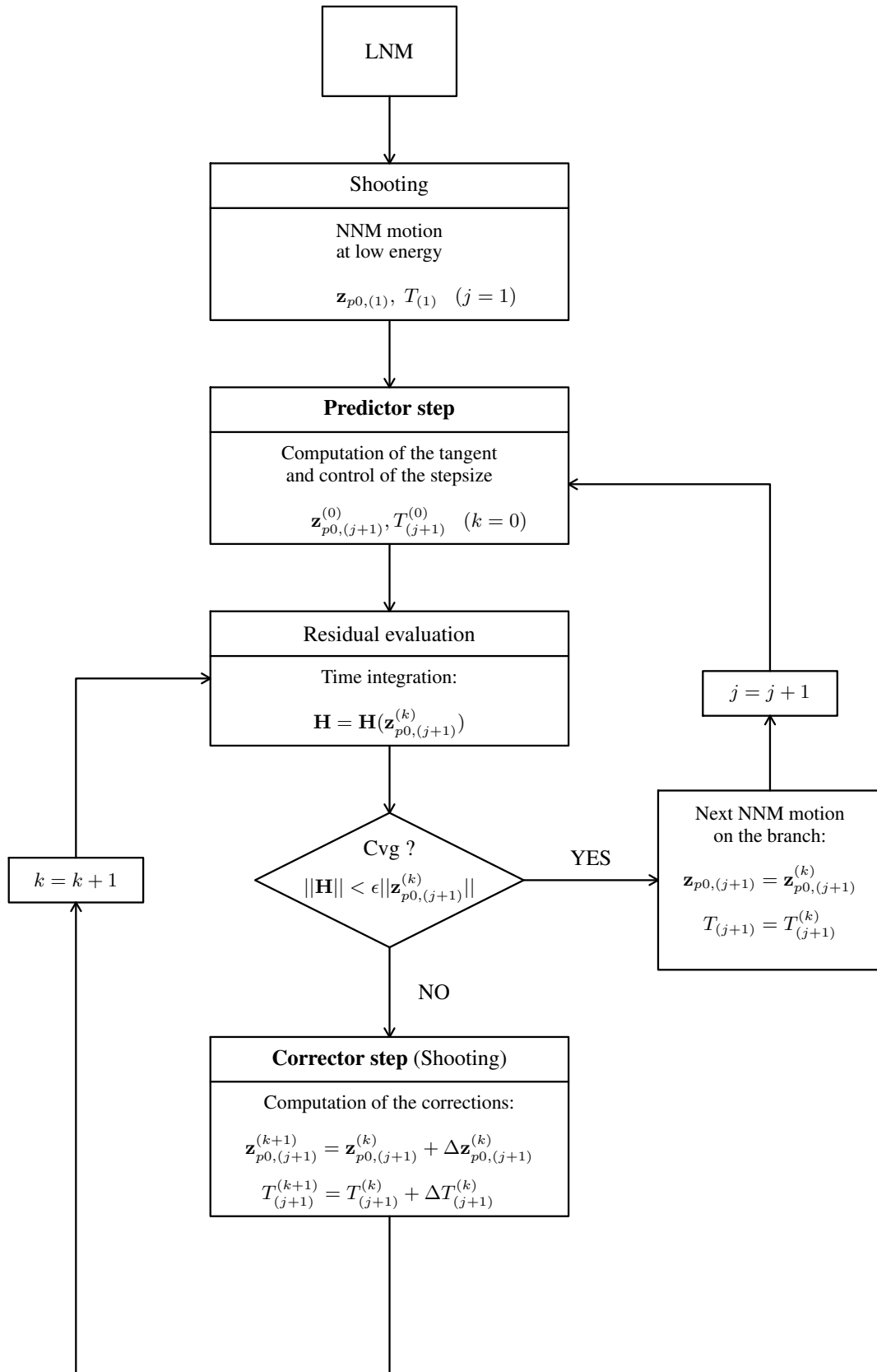


Figure 1. Algorithm for NNM computation.

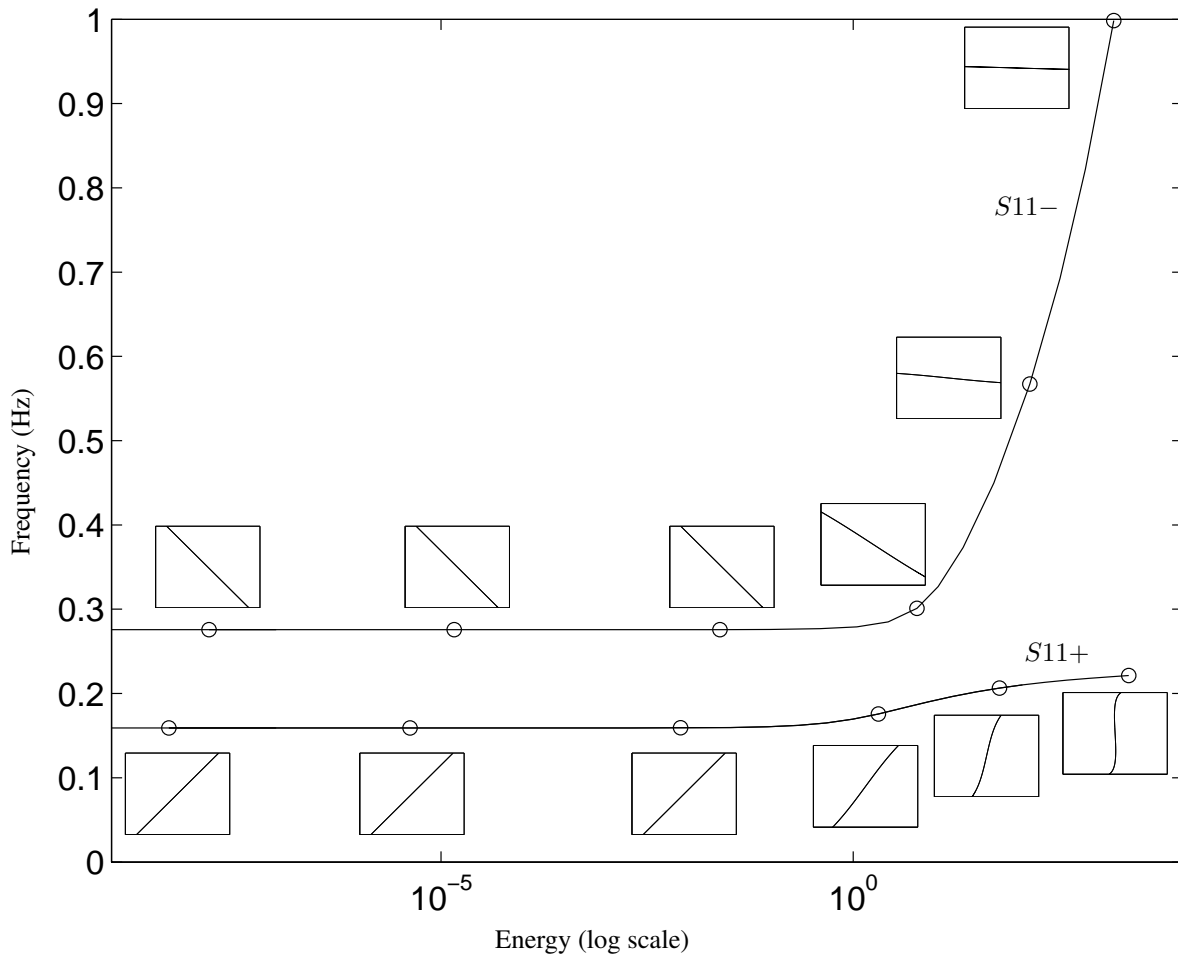


Figure 2. Frequency-energy plot of the 2DOF system computed with the proposed numerical method. NNM motions depicted in the configuration space are inset. The horizontal and vertical axes in these plots are the displacements of the first and second DOFs, respectively; the aspect ratio is set so that increments on the horizontal and vertical axes are equal in size to indicate whether or not the motion is localized to a particular DOF.

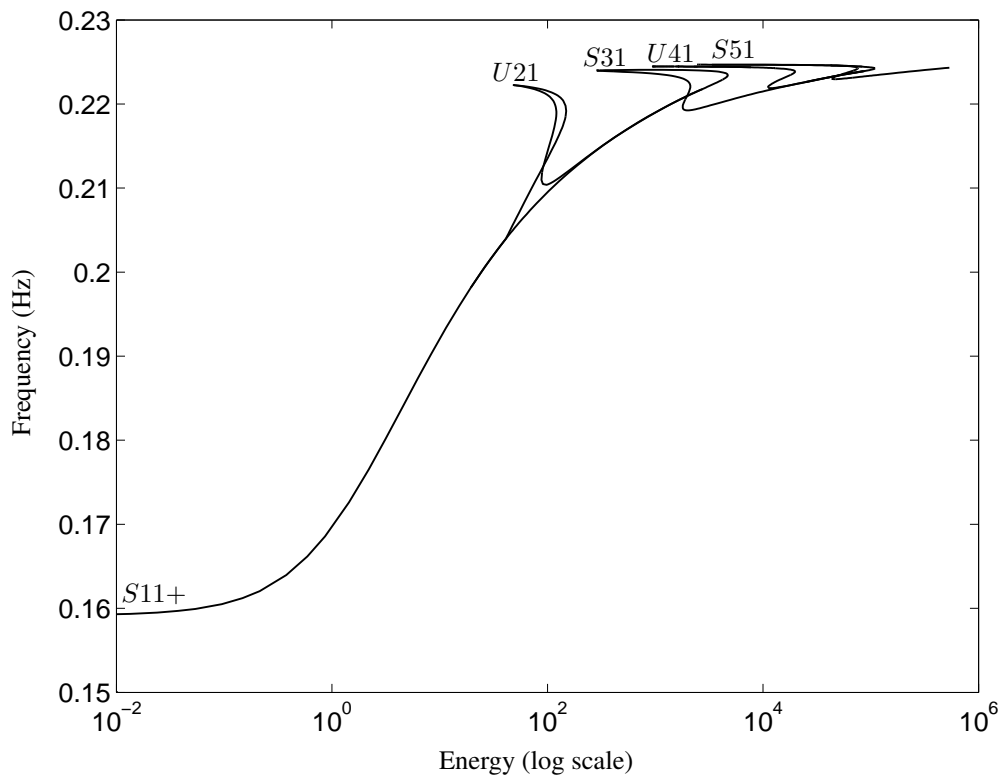


Figure 3. $S11+$ at higher energy levels and internally resonant NNMs ($U21$, $S31$, $U41$, $S51$).